

Physical and dielectric properties of $\text{Bi}_{4-x}\text{R}_x\text{Sr}_3\text{Ca}_3\text{Cu}_2\text{O}_{10}$ glasses ($x = 0.5$ and $\text{R} = \text{Ag}, \text{Ni}$)

A. MEMON, D. B. TANNER

Department of Physics, University of Florida, Gainesville, FL 32611

E-mail: aman@phys.ufl.edu

The reflectivity spectra of semiconducting $\text{Bi}_4\text{Sr}_3\text{Ca}_3\text{Cu}_2\text{O}_{10}$ glasses were measured over the frequency range between 100 and 4000 cm^{-1} , and were analysed using Kramer-Kronig routines. It is observed that the static and high frequency dielectric constant varies as the bismuth is partially replaced by silver and nickel. The X-ray diffraction and the dc resistivity measurements shows a semiconducting behaviour for all the samples. The measured values of the activation energy and other physical parameters based on infrared reflectance measurements are consistent with published work on the similar materials, the activation energy W , hopping energy W_H and other physical parameters vary with the nickel and silver substitutions. It is shown that the hopping in these materials occurs in non-adiabatic regime, unlike other transition metal oxide glasses. © 1999 Kluwer Academic Publishers

1. Introduction

Transition metal oxides, such as V_2O_5 , MoO_3 , CuO , and TiO_2 , when heated with glass forming substances like P_2O_5 , TeO_2 , and GeO_2 form semiconducting oxide glasses. One condition for semiconducting behavior is that the transition metal ions should be capable of existing in more than one valence state. Electrical conduction in these glasses occurs by electron hopping from an ion of the low valence state V^{4+} transition metal to an ion of the high valence state V^{5+} [1–3]. According to [4] a strong electron-lattice interaction exists in these semiconducting oxide glasses which causes the formation of small polarons and hence the conduction due to hopping of small polarons between the transition metal ions of two different valence states. Soon after the discovery of the high T_c superconducting phases of the BiSrCaCuO system [6] it was shown that certain compositions readily form glasses [6–8]. These glasses with transition metal ions are very useful precursor materials for the processing of diverse geometry such as oxide wires, tapes, or thin films. The existence of small polarons in these types of materials has been discussed by various groups [9–11]. Photoinduced doping of insulating samples have indicated that the charge carriers produced by this method are localized small polarons. The appearance of these charge carriers is accompanied by a shift of Raman or infrared active local phonon modes. It is observed that the shift in phonon frequency for the photo-doped insulator and the chemically-doped metallic sample is identical thus indicating that the charge carriers in the metallic phase are small polaron.

Infrared spectroscopy has been extensively employed to investigate the vibrational and structural properties of glasses [12–16]. It is well known that the

infrared or Raman spectra of glasses consist of excitations very similar to those of crystals with similar composition, with the difference that the linewidth of glass spectra is large compared to that of the crystals. This work offers the first systematic reflectance study of $\text{Bi}_4\text{Sr}_3\text{Ca}_3\text{Cu}_2\text{O}_{10}$ glasses. A major portion of the paper is related to the extraction of the values for hopping energy, activation energy, and other physical parameters based on infrared reflectance studies. Analysis of these measurements provides the frequency-dependent dielectric response function, and the values of characteristic phonon frequencies [13]. The effective dielectric constant obtained from Kramer-Kronig is used with Mott and Austin and Mott theory [1–4] to obtain the activation energy and other related physical parameters.

2. Experimental

2.1. Sample preparation

Stoichiometric amounts of Bi_2O_3 , SrCO_3 , CaCO_3 , AgO , NiO_2 and CuO were mixed in appropriate quantities and calcined at 800 °C for 10 h in air. The calcined powders were ground several times in a mortar and pestle during 10 h heat treatment and then melted in an alumina crucible at 1250 °C for about 1 h in an electric furnace. The melt was poured onto a stainless steel block and pressed quickly to a thickness of about 3 mm by placing a steel block on the melt. Three samples were made using the above method with the following compositions: Sample no. 1, $\text{Bi}_4\text{Sr}_3\text{Ca}_3\text{Cu}_2\text{O}_{10}$; sample no. 2, $\text{Bi}_{3.5}\text{Ag}_{0.5}\text{Sr}_3\text{Ca}_3\text{Cu}_2\text{O}_{10}$ and sample no. 3, $\text{Bi}_{3.5}\text{Ni}_{0.5}\text{Sr}_3\text{Ca}_3\text{Cu}_2\text{O}_{10}$. These samples were

polished optically flat for the reflectance measurements in the different spectral range. The X-ray diffraction measurements performed with $\text{CuK}\alpha$ radiation between 2θ values of 20° and 60° do not show any structure, indicating that all three samples are in the amorphous semiconducting state. The dc resistivity measurements shows a semiconducting behaviour of these samples. The resistivity of sample no. 1 is very high and reduces slightly on doping. These observations are consistent with the IR measurements. The reflectance measurements were performed over a frequency region between 80 and 4000 cm^{-1} using a Bruker IFS-113v fast scanning Fourier transform spectrometer which covers the far-infrared and mid-infrared region. The measurements were performed at room temperature using a highly sensitive liquid helium cooled bolometer.

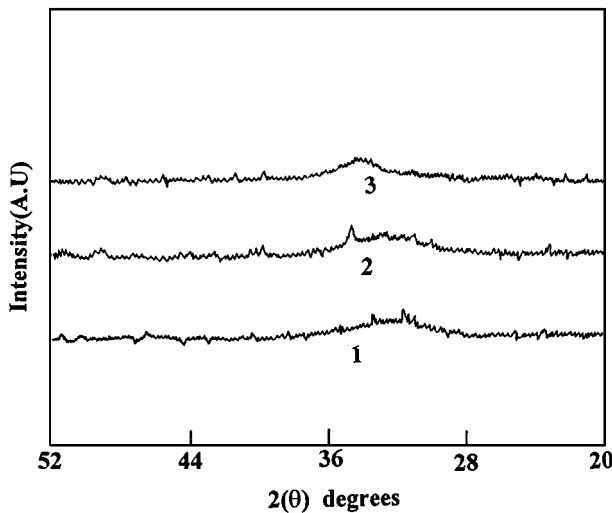


Figure 1 X-ray diffraction pattern of $\text{Bi}_{4-x}\text{R}_x\text{Sr}_3\text{Ca}_3\text{Cu}_2\text{O}_{10}$ glasses (here $x=0$, for sample 1, and $x=0.5$ and $\text{R}=\text{Ag}, \text{Ni}$ for samples 2 and 3, respectively).

3. Optical properties

3.1. Reflectance measurements

The X-ray diffraction spectra are shown in Fig. 1. All the three glass samples are featureless except for a small hump at about 30° . The scattering wave vector k is obtained from the relation $k = 4\pi \sin \theta / \lambda$ has a value of $2.09/\text{\AA}$, which is a representative value for an amorphous material. Thus all three samples are amorphous semiconductors. The measured reflectance spectra for all the samples are shown in Fig. 2. From this figure we observed that the reflectance of the parent sample in the far-infrared region reduces as the bismuth is partially substituted, which indicates that the number of free carriers reduces on the partial substitution at the bismuth site; this could be due to the loss of oxygen on doping. From Fig. 2 we also observe that the reflectance minima for the three samples is not effected by the doping. The mid-infrared response of sample 2 i.e., silver substituted at the bismuth site shows an increase in the reflectance, where as nickel substituted sample shows a drop in the mid-infrared reflectance.

The experimental reflectivity data were analyzed using Kramer-Kronig relations. From the measured reflectance spectra we obtained the frequency dependent dielectric functions, absorption coefficient, and optical conductivity. Since this method requires the knowledge of reflectivity as a function of frequency from zero to infinity, extrapolations had to be used. At low frequencies, the reflectance is assumed to be constant; at high frequencies R was continued smoothly until about $50,000\text{ cm}^{-1}$ and then made to go as $(\omega)^{-4}$. At first the measured reflectance $R(\omega) = r^2$ is transformed to obtain the phase angle difference $\theta(\omega)$ between reflected and incident wave i.e.,

$$\theta(\omega) = \int_0^\infty \frac{\ln R(\omega') d(\omega')}{\omega^2 - \omega'^2} \quad (1)$$

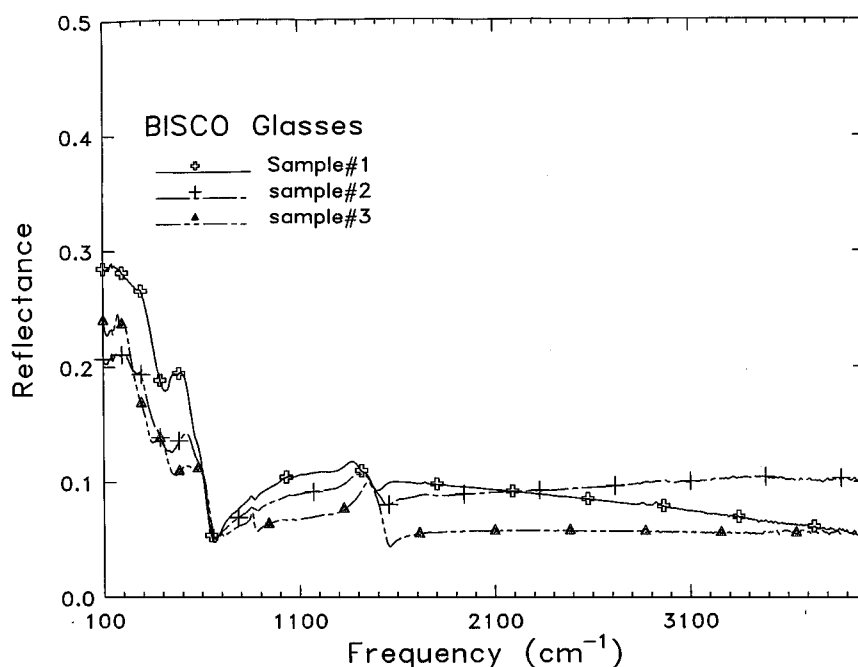


Figure 2 Infrared reflectance spectra of $\text{Bi}_{4-x}\text{R}_x\text{Sr}_3\text{Ca}_3\text{Cu}_2\text{O}_{10}$ glasses (here $x=0$, for Sample 1 and $x=0.5$ and $\text{R}=\text{Ag}, \text{Ni}$ for samples 2 and 3, respectively).

The real and imaginary parts of the dielectric function $\epsilon_1(\omega)$ and $\epsilon_2(\omega)$ are related to the reflectivity $r(\omega)$ and $\theta(\omega)$ through the complex refractive index, $N = n + ik$ as

$$n(\omega) = \frac{1 - r^2}{1 + r^2 - 2r \cos \theta} \quad (2)$$

$$k(\omega) = \frac{2r \cos \theta}{1 + r^2 - 2r \cos \theta} \quad (3)$$

Also, the real and imaginary parts of the dielectric function are related to $n(\omega)$ and $k(\omega)$ as

$$\epsilon_1(\omega) = n^2(\omega) - k^2(\omega), \quad (4)$$

and

$$\epsilon_2(\omega) = 2nk, \quad (5)$$

The optical dielectric constants are then used to calculate the real part of the optical conductivity and the frequency dependent absorption coefficient, as

$$\sigma_1 = \frac{\omega \epsilon_2}{4\pi} \quad (6)$$

and

$$\alpha = (4\pi \nu k d) \quad (7)$$

The functions $\epsilon_1(\omega)$, $\alpha(\omega)$, and $\sigma_1(\omega)$ are shown in Figs 3–5, respectively. In infrared region the real part

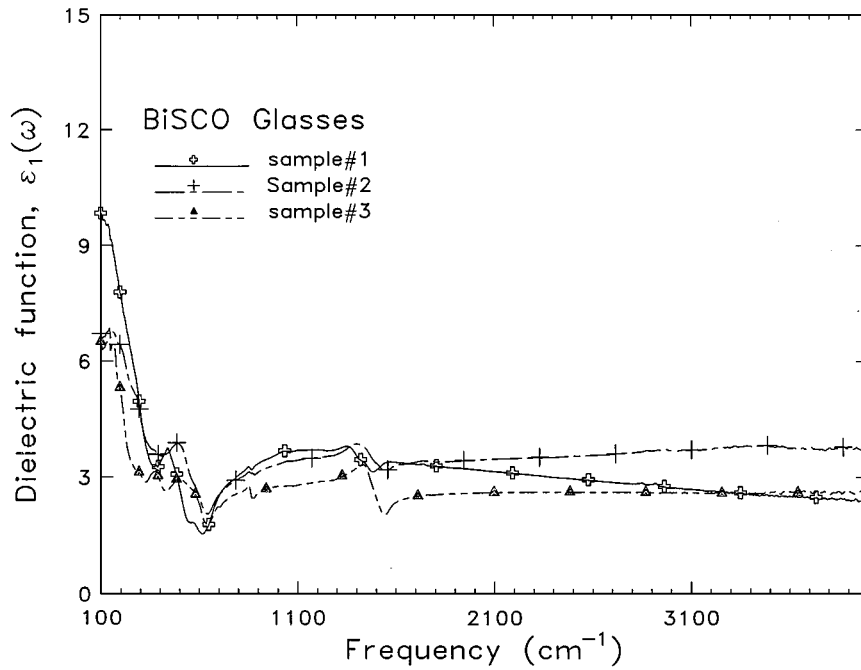


Figure 3 The real part, $\epsilon_1(\omega)$ of the dielectric function for samples 1, 2 and 3.

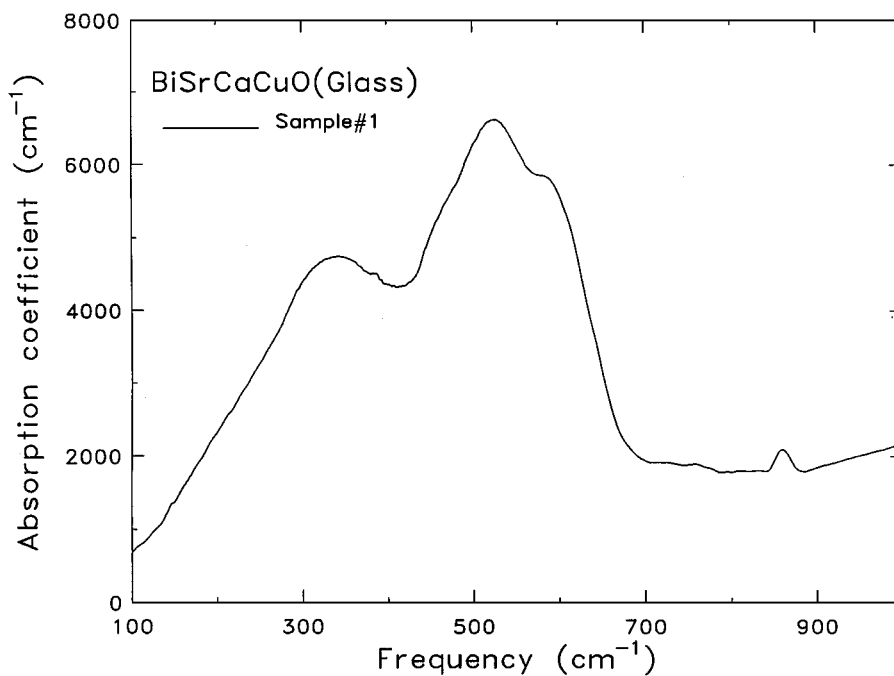


Figure 4 The absorption coefficient $\alpha(\omega)$, versus frequency for sample 1.

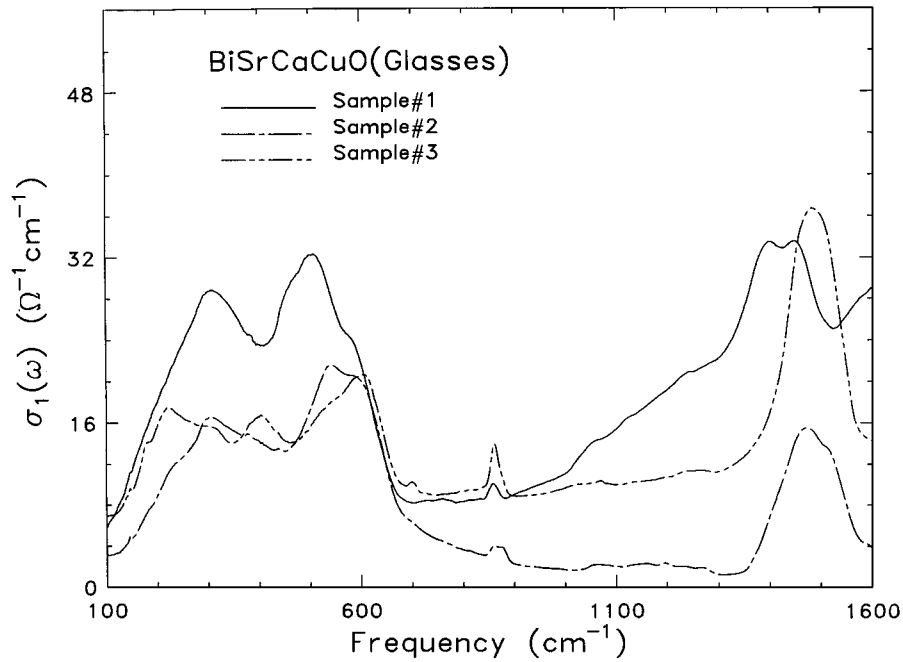


Figure 5 Optical conductivity function, $\sigma_1(\omega)$ for the samples 1, 2 and 3.

of dielectric response function is highly frequency dependent which indicates that the loss mechanism must have a distribution of relaxation time rather than a single relaxation time. This phenomenon is similar to those of other transition metal oxides studied at ambient temperature. As there is no strong absorption at high frequencies in this material, the value of $\epsilon_1(\omega)$ attains a constant value, which leads to an estimate of the high frequency dielectric constant ϵ_∞ . For the calculation of polaron binding energy, the effective dielectric constant (ϵ_p) can be approximated by $(\epsilon_p) = \epsilon_\infty = N^2$, provided (ϵ_0) is very large as compared to ϵ_∞ if the value of ϵ_0 is not large enough then one can use the relation:

$$\frac{1}{\epsilon_p} = \left(\frac{1}{\epsilon_\infty} - \frac{1}{\epsilon_0} \right) \quad (8)$$

The values of ϵ_p , the effective dielectric constant obtained from Fig. 3, are listed in Table II. The substitution of silver and nickel at the bismuth site increases the values of effective dielectric constants, ϵ_p , and hence is responsible for the change in the activation energy and the microstructure of these glasses. The value of the characteristic phonon frequency, estimated from absorption spectra of Fig. 4, is slightly higher than those reported in literature and increases on doping. The optical conductivity is represented by Fig. 5; the conductivity of the pure sample reduces on doping. The details of vibrational features observed in conductivity spectra are discussed in Section 3.3.

3.2. Discussion

In transition metal oxides glasses, strong interaction between the unpaired electrons and lattice leads to the polarization of the lattice and displacement of the oxygen ions away from the low-valence transition metal ions. This localization process is sufficient to produce a small polaron. The theory of the small polaron has

been discussed in detail by Mott [4] and Austin and Mott [1]. Using the polaron hopping mechanism as described by the above authors, the activation energy W , can be expressed as

$$W = W_H + \frac{W_D}{2} \quad (9)$$

where W_H and W_D are the polaron hopping and disorder energy arising from the energy difference of the neighbouring sites. The value of W_H is calculated using the relation:

$$W_H = \frac{W_P}{2} = \frac{e^2}{4\epsilon_p} \left(\frac{1}{r_p} - \frac{1}{R} \right) \quad (10)$$

Where W_P , e , ϵ_p , r_p and R are respectively the polaron hopping energy, the charge of the electron, measured effective dielectric constant, the polaron radius and finally R which is the mean distance between transition metal ions. The polaron radius r_p used in Equation 9 has been estimated by several authors [1, 17] as

$$r_p = \frac{1}{2} \left[\frac{\pi}{6N} \right]^{1/3} \quad (11)$$

where N is the concentration of Cu ions in the glass, which is obtained from the derived formula and the measured values of density, calculated from Archimede's principle. In contrast, the value of R in Equation 9 is determined from the composition found by chemical analysis and density measurements. The disorder energy W_D in Equation 8 is calculated from Miller and Abraham's theory [18] using the equation,

$$W_D = \frac{Ke^2}{\epsilon_0 R} \quad (12)$$

Here ϵ_0 is the static dielectric constant obtained from Kramer-Kronig analysis of the reflectance data, K is the constant of the order of 0.3 and e is the electronic

TABLE I Some physical parameters of the BSCCO glasses

Sample no.	Dopant	ρ (g cm ⁻³)	$N \times 10^{21}$ (cm ³)	R (Å)	r_p (Å)
1	—	5.98	3.47	6.65	2.63
2	Ag	5.92	3.86	6.37	2.56
3	Ni	5.84	3.92	6.34	2.55

TABLE II Measured values of effective dielectric constant and the activation energy

Sample no.	Dopant	ϵ_p	W_H (eV)	W_D (eV)	W_P (eV)	W (eV)	γ_p
1	—	3.00	0.274	0.0127	0.546	0.28	8.5
2	Ag	3.81	0.12	0.020	0.24	0.13	4.5
3	Ni	3.21	0.262	0.0118	0.524	0.268	8.1

TABLE III Vibrational modes in BSCCO glasses measured in cm⁻¹

Sample no.	1	2	3	4	5
1	303	505	858	1402	1452
2	305	535	860	—	1470
3	223/303	598	856	—	1476

charge. Some physical parameters for pure and doped BiSrCaCuO glasses, such as ρ , N , r_p , W , W_H , W_D , W_P and (ϵ_p) are listed in Tables I and II, respectively. The observed values are in agreement with published data [7] for such materials. The condition for small polaron is

$$J \leq \frac{W_H}{3} \quad (13)$$

where J is the polaron bandwidth and W_H is hopping energy. Once J is shown to satisfy Equation 13 and so is in accord with the formation of the small polaron, then the other physical properties of glass can be calculated. The polaron coupling constant γ_p can be calculated from the relation between characteristic phonon frequency and the polaron binding energy [1] as,

$$\gamma_p = \frac{W_P}{h\nu_{ph}} \quad (14)$$

The measured value of the characteristic phonon frequencies for sample 1 obtained from the absorption spectrum in Fig. 4 is 520 cm⁻¹; this is in agreement with the one reported in Ref. [7] measured by infrared absorption, but is slightly higher than the values obtained from conductivity measurements. The coupling constant obtained after substituting the calculated values of W_P and characteristic phonon frequency in Equation 14 is about 8.5. Austin and Mott have suggested that a value for $\gamma_p > 4$ usually indicates strong electron phonon interaction in solids. Our calculated values of γ_p are greater than 4 which indicates a strong electron phonon interaction in BSCCO materials. The calculated values of γ_p are listed in Table II. We obtain the polaron bandwidth J_p from

$$J_p = \frac{J}{2} = h\nu_{ph} \exp(-\gamma_p) \quad (15)$$

For non-adiabatic hopping the polaron bandwidth is $J < H$ where H is given by

$$H = \left(\frac{2K_B T W_H}{\pi} \right)^{1/4} (h\nu_{ph}\pi)^{1/2} \quad (16)$$

and J_p from Equation 15. We obtain the value of H as 37 meV which is much higher than that of J_p , i.e., 7.0 meV, calculated from Equation 15, because $J \ll H$ we conclude that the hopping phenomena in these glasses occurs in the non-adiabatic regime.

3.3. Vibrational features

Fig. 4 represents the infrared conductivity of all the three glasses. It is apparent that as the bismuth is substituted by the silver and nickel the conductivity of the material is reduced in the infrared region, indicating that the doped samples are inclined towards more disordered state and hence have larger activation energy. All the three glasses have four to six major vibrational features in the measured frequency range. Crystalline Bi₂O₃ has absorption peaks around 510, 600 and 1400 cm⁻¹; these peaks are also retained in some of the glasses. All the three samples show an absorption band around 860 and 1470 cm⁻¹ which may be due to the presence of Sr and CaCO₃ in the samples. In the nickel doped sample two new peaks appear at 217 and 404 cm⁻¹ and the peaks at 303, 505 and 1450 cm⁻¹ shift towards higher frequencies side. This shift could be due to the large difference between the atomic masses of bismuth and the nickel. In contrast, the substitution of silver at the bismuth site leads to a small shift in the vibrational frequencies. These shifts could also be due to appearance of charge carriers which causes shifts in Raman and infrared phonon modes [10]. A common effect of both the dopants is to reduce the optical conductivity. We did not observe any hydroxyl mode reported by [7] between 3500–3700 cm⁻¹ in our spectra. It appears that since the earlier samples were made by mulling technique, where small portion of glass powder is dispersed in a transparent matrix such as KBr. These procedures may have certain undesirable effects such as Christian effect, i.e., dispersion at high frequencies, loss of spectral intensity and band shape and residual water from mulling agent KBr, which is hygroscopic in nature.

4. Conclusions

The present studies of BSCCO glasses shows that the glasses made are semiconducting in nature and that the optical conductivity of these glasses reduced considerably on the substitution of nickel and silver at the bismuth site, whereas the activation energy W of the samples 2 and 3, increases as compared to sample 1. The measured larger values of γ_p for our glasses indicate that a strong electron-lattice interaction exist in these materials and hence confirms the formation of small polarons as predicted by the theories. Finally, the conduction in BSCCO glasses is found to be due to hopping of small polarons between the localized states and the

hopping process occurs in a non adiabatic regime unlike the other transition metal oxides.

Acknowledgement

This work was supported by National Science Foundation grant no. DMR-9705108.

References

1. I. G. AUSTIN and N. F. MOTT, *Adv. Phys.* **18** (1969) 41.
2. L. MURAWSKI, C. H. CHUNG and J. D. MACKENZIE, *J. Non-Cryst. Solids* **32** (1979) 208.
3. M. SAYER and MANSING, *Phys. Rev.* **B6** (1972) 467.
4. N. F. MOTT, *J. Non-Cryst. Solids* **1** (1968).
5. H. MAEDA, T. TANAKA, M. FUKUTOMI and T. ASANO, *Jpn. J. Appl. Phys.* **27** (1988) L209.
6. S. KOMATSU, R. SATO, K. IMAI, K. MATSUHITA and T. YAMASHITA, *ibid.* **27** (1988) L550.
7. S. MOLLAH, K. K. SOM, K. BOSE, A. K. CHAKRAVORTY and B. K. CHAUDHARI, *Phys. Rev.* **B46** **17** (1992) 11075.
8. H. ZHENG and J. D. MACKENZIE, *Phys. Rev.* **38** (1989) 7166.
9. H. ZHENG, M. W. COLBY and J. D. MACKENZIE, *J. Non-Cryst. Solids* **127** (1991) 143.
10. J. WONG and C. A. ANGELL, "Glass Structure by Spectroscopy" (Dekker, New York, 1976) chap. 7.
11. F. GERVAIS, A. BLIN, D. MASSIOT, J. P. COUTURES, M. H. CHOPINET and F. NAUDIN, *J. Non-Cryst. Solids* **89** (1987) 384.
12. F. L. GALEENER, A. J. LEADBETTER and M. W. STRINGFELLOW, *Phys. Rev. B.* **27**(2) (1983) 1052.
13. F. WOOTWEN, "Optical Properties of Solids" (Academic Press, New York, 1972).
14. C. A. ANGELL, *Solid Stat Ionics* **18/19** (1986) 72.
15. G. N. GREAVES, *ibid.* **11** (1973) 427.
16. A. MEMON, M. N. KHAN, S. AL DALLAL and D.B. TANNER *J. Mater. Sci.* **30** (1995) 5991.
17. V. N. BOGMOLOV, E. K. KUDINOV and YU. A. FKISOV, *Sov. Phys. Solid-State* **9** (1968) 2502.
18. A. MILLER and E. ABRAHAMAS, *Phys. Rev.* **120** (1969) 745.

Received 11 November 1998
and accepted 8 February 1999